

Controlled-Z gates with giant atoms in structured waveguides

Walter Rieck,^{1,2} Ariadna Soro,¹ Anton Frisk Kockum,^{1,*} and Guangze Chen^{1,†}

¹*Department of Microtechnology and Nanoscience,
Chalmers University of Technology, 41296 Gothenburg, Sweden*

²*Department of Physics, Stockholm University, 10691 Stockholm, Sweden*

(Dated: March 30, 2026)

Giant atoms are quantum emitters coupled to waveguides at multiple, spatially separated points, enabling interference effects that fundamentally change their light–matter interactions. A notable consequence of the interference is the emergence of decoherence-free interaction (DFI), which allows coherent excitation exchange between giant atoms via the waveguide without radiative loss. Leveraging DFI offers a promising route to implementing two-qubit quantum gates without the need for additional resources, positioning giant atoms as a versatile platform for scalable universal quantum simulators. However, existing work has focused primarily on continuous, Markovian waveguides; in structured waveguides, where non-Markovian effects become significant, only iSWAP gates have been explored. To address this gap, we introduce and analyze a protocol for implementing controlled-Z (CZ) gates with giant atoms in structured waveguides. We first show that while a minimal two-point coupling scheme supports DFI, it also exhibits strong non-Markovian effects that substantially degrade gate fidelity. To overcome this limitation, we propose an extended design featuring a third coupling point. This configuration suppresses non-Markovian effects and enables CZ gates with fidelities up to 97.7% (assuming typical values for experimental imperfections). Our results broaden the accessible gate set for giant atoms in structured waveguides to include both iSWAP and CZ gates, advancing these systems as a pathway toward universal quantum simulators operating in non-Markovian environments.

I. INTRODUCTION

Universal quantum simulators are powerful tools for exploring complex open quantum many-body dynamics [1–3]. Yet, most existing quantum simulators are optimized for implementing only specific two-qubit gates [3–5]. Although this can be sufficient for realizing a universal gate set together with single-qubit gates, it is generally desirable to have more flexibility regarding which two-qubit gates one can implement, e.g., to reduce the depth of quantum circuits. However, enabling such flexibility typically requires additional coupling elements [6–20] or complicated drive schemes [21–26] that limit the feasibility of building large-scale quantum simulators.

Here, we explore how an extended set of two-qubit gates can be realized using giant atoms (GAs) [27–31], which have recently emerged as a versatile platform for scalable universal quantum simulators that can handle open quantum systems [32–35]. Unlike conventional small atoms that interact locally, GAs couple to waveguides at multiple, spatially separated points. This non-local coupling results in interference-driven light–matter dynamics, giving rise to qualitatively new phenomena such as frequency-dependent decay [29, 31, 36, 37], directional emission [38–41], tunable interaction rates [30, 31, 37] between distant GAs, and much more [27, 42–74]. Among the most striking consequences of this nonlocal coupling is the possibility of realizing decoherence-free interactions (DFIs), where two or more atoms exchange

excitations coherently while completely suppressing radiative decay through destructive interference between coupling points [30, 31]. These DFIs provide a natural mechanism for entangling gates without the need for additional parametric couplers, making GAs a versatile platform for quantum simulators [32–35].

Previous studies have often focused on GAs coupled to continuous waveguides, whose dispersion can be approximated as linear in the frequency regime where the atoms operate. In these setups, the Markovian approximation is typically valid and analytical treatments are tractable [32, 34, 35]. Additionally, in such setups, iSWAP gates have been experimentally demonstrated using superconducting qubits coupled to a microwave waveguide [31].

In contrast to continuous waveguides, structured waveguides [75–77], such as coupled-cavity arrays [41, 78–80] or photonic crystals [81–83], have nonlinear dispersions with band edges and gaps in the frequency regime where the atoms operate. Exploring GAs coupled to structured waveguides thus opens up the possibility of exploiting band-edge effects, engineered dispersion, and strong non-Markovian effects [48, 51, 55, 84–97]. Yet, since the Markovian approximation does not hold, such studies require keeping track of the whole system’s dynamics and have thus mainly focused on single-excitation dynamics, which only support iSWAP gates [55]. Establishing universal quantum simulators in GAs coupled to structured waveguides would benefit from additional entangling gates such as the controlled-Z (CZ) gate, which remains to be explored as it relies on dynamics in the two-excitation sector.

In this article, we propose and analyze a protocol for

* anton.frisk.kockum@chalmers.se

† guangze@chalmers.se

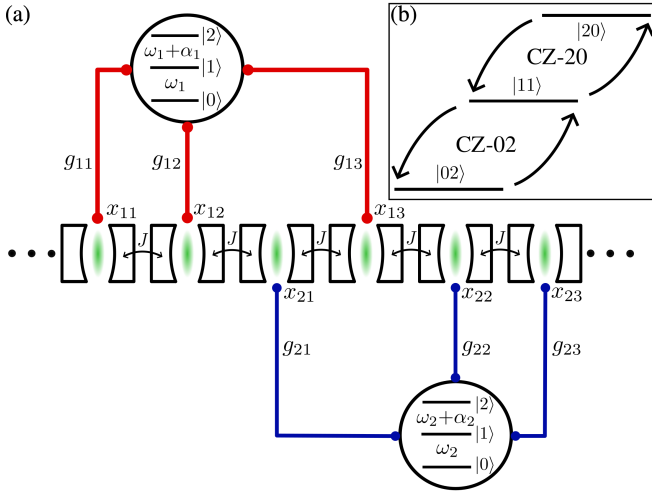


FIG. 1. Model and gate scheme. (a) Schematic of two giant atoms (GAs) coupled to a one-dimensional array of coupled cavities with nearest-neighbor hopping rate J . Each atom m is connected with coupling strength g_{mj} to the array at site x_{mj} . The atoms have distinct transition frequencies $\omega_{1(2)}$ and anharmonicities $\alpha_{1(2)}$. (b) The CZ gate in GAs can be implemented via the pathway CZ-02 (CZ-20), which coherently transfers the population of the $|11\rangle$ state to the $|02\rangle$ ($|20\rangle$) state and then brings it back, accumulating a π phase shift.

implementing a CZ gate between two GAs coupled to a structured waveguide. We begin by studying the minimal two-point coupling configuration, which supports DFI, but suffers from non-Markovian effects that strongly degrade the DFI. We then demonstrate that introducing a third coupling point shifts the decoherence-free frequencies closer to the center of the photonic band of the structured waveguide, thereby mitigating these effects. For experimentally realistic parameters in superconducting qubits, we show that this design yields CZ gate fidelities up to 97.7%. These results equip GAs coupled to structured waveguides with an extended gate set involving both iSWAP and CZ gates, pushing these platforms forward toward universal quantum simulators in non-Markovian environments.

The rest of this article is organized as follows. In Section II, we introduce the model of two three-level GAs coupled to a structured waveguide. In Section III, we analyze the CZ gate protocol, beginning with the minimal two-point configuration and then extending to the improved three-point scheme. We further evaluate the resulting gate fidelity and discuss experimental feasibility. Finally, in Section IV, we summarize the main findings and outline their broader implications.

II. MODEL AND METHOD

A. System Hamiltonian

We consider a system of two GAs coupled to a one-dimensional structured waveguide, as shown in Fig. 1(a). The total Hamiltonian for this system is given by

$$H = H_A + H_B + H_{\text{int}}, \quad (1)$$

where H_A describes the bare GAs, H_B describes the bare bath (i.e., the waveguide), and H_{int} describes the interaction between the atoms and the bath. Since the CZ gate dynamics in our scheme involve the $|2\rangle$ level of the qubits [see Fig. 1(b)], we model each atom as a three-level system ($\hbar = 1$ here and in the rest of the article):

$$H_A = \sum_{m=1}^2 \left[(2\omega_m + \alpha_m) \frac{\sigma_m^{(2),+} \sigma_m^{(2),-}}{2} + \omega_m \sigma_m^{(1),+} \sigma_m^{(1),-} \right], \quad (2)$$

where ω_m denotes the transition frequency from the ground state to the first excited state for atom m , α_m denotes the anharmonicity of atom m , and the ladder operators are defined as

$$\sigma_m^{(j),+} |j-1\rangle_m = \sqrt{j} |j\rangle_m, \quad \sigma_m^{(j),-} |j\rangle_m = \sqrt{j} |j-1\rangle_m. \quad (3)$$

We model the structured bath as a one-dimensional array of N coupled cavities, with the center of the photonic band at the frequency ω_c :

$$H_B = \sum_{n=1}^N \omega_c a_n^\dagger a_n - J \sum_{n=1}^{N-1} (a_n a_{n+1}^\dagger + \text{H.c.}), \quad (4)$$

where J is the coupling rate between adjacent cavities, a_n and a_n^\dagger are the annihilation and creation operators, respectively, for photons in cavity n , and H.c. denotes the Hermitian conjugate. This Hamiltonian yields the dispersion relation

$$\omega(k) = -2J \cos k + \omega_c, \quad (5)$$

where k is the wave number, resulting in a cosine band of width $4J$. As ω_c is a constant, we can go to a frame rotating at that frequency in Eq. (1) such that the first term in Eq. (4) is zero and we redefine $\omega_m = \omega_m - \omega_c$ in Eq. (2).

Under the rotating-wave approximation, the interaction Hamiltonian between the atoms and the bath takes the form

$$H_{\text{int}} = g_{mj} \sum_{m=1}^2 \sum_{j=1}^{p_m} \left[\sigma_m^{(1),+} a_{x_{mj}} + \sigma_m^{(2),+} a_{x_{mj}} + \text{H.c.} \right], \quad (6)$$

where x_{mj} denotes the position of the j th coupling point of atom m and g_{mj} the corresponding coupling strength. Each atom is coupled to p_m cavities in total.

B. Numerical approach to dynamics

Solving the full Hamiltonian H in Eq. (1) is computationally challenging, as it acts on an infinite-dimensional Hilbert space. However, since H conserves the total excitation number of the atom–bath system, it can be projected onto subspaces with a fixed number of excitations. In particular, the dynamics of the iSWAP gate only involve single-excitation states, and the problem can therefore be solved by restricting the Hamiltonian to the single-excitation subspace. In contrast, the dynamics of the CZ gate involve two excitations, going beyond the single-excitation regime that is typically studied in giant-atom systems [55]. As a result, we must numerically simulate the system in the two-excitation subspace. This subspace is spanned by the states

$$\begin{aligned} |20\rangle_A \otimes |0\rangle_B, & \quad |11\rangle_A \otimes |0\rangle_B, \\ |02\rangle_A \otimes |0\rangle_B, & \quad |10\rangle_A \otimes |j\rangle_B, \\ |01\rangle_A \otimes |j\rangle_B, & \quad |00\rangle_A \otimes |jk\rangle_B, \end{aligned} \quad (7)$$

where $|n_1, n_2\rangle_A$ denotes the state of the two atoms with excitation numbers $n_{1,2} \in \{0, 1, 2\}$, $|0\rangle_B$ is the vacuum state of the waveguide, $|j\rangle_B$ represents a single photon in cavity j , and $|jk\rangle_B$ corresponds to two photons in the waveguide—one in cavity j and one in cavity k ($j = k$ covers the case of two photons in one cavity). Since the photons are bosons, we impose the symmetry condition $|jk\rangle_B = |kj\rangle_B$. Using this basis, we project the full many-body description from the Hamiltonian in Eq. (1) onto the two-excitation subspace and simulate the system dynamics accordingly.

C. Computing gate fidelity

The average gate fidelity of the CZ gate F_{CZ} is related to the process fidelity \mathcal{F}_{CZ} by

$$F_{\text{CZ}} = \frac{d\mathcal{F}_{\text{CZ}} + 1}{d + 1}, \quad (8)$$

where $d = 4$ is the Hilbert-space dimension of the computational subspace for the two-qubit CZ gate [98].

To evaluate \mathcal{F}_{CZ} , we first describe the state of the total system as

$$|\psi\rangle = \sum_{m,n} \alpha_{mn} |m\rangle_A \otimes |n\rangle_B, \quad (9)$$

where $|m\rangle_A$ and $|n\rangle_B$ denote atomic and bath states, respectively [see Eq. (7)]. The corresponding density matrix is

$$\rho_{\text{tot}} = \sum_{m,n} \sum_{m',n'} \alpha_{mn} \alpha_{m'n'}^* |m\rangle_A \langle m'|_A \otimes |n\rangle_B \langle n'|_B. \quad (10)$$

Tracing out the bath degrees of freedom gives the reduced atomic density matrix

$$\rho_A = \text{Tr}_B \rho_{\text{tot}} = \sum_{m,m',n} \alpha_{mn} \alpha_{m'n}^* |m\rangle_A \langle m'|_A. \quad (11)$$

Since the computational subspace only involves the atomic states $\{|11\rangle, |10\rangle, |01\rangle, |00\rangle\}$, we can compute ρ_A as the product of a matrix M with its conjugate transpose,

$$M_{mn} = \begin{cases} \alpha_{mn}, & \text{if } |m\rangle_A |n\rangle_B \in \text{basis,} \\ 0, & \text{otherwise,} \end{cases} \quad \rho_A = MM^\dagger. \quad (12)$$

Using this reduced density matrix, a process \mathcal{E} can be represented by its Choi matrix [99]

$$\Phi = \sum_{m,n=11,10,01,00} |m\rangle \langle n| \otimes \mathcal{E}(|m\rangle \langle n|), \quad (13)$$

where $|m\rangle, |n\rangle$ runs over the computational basis states and $\mathcal{E}(|m\rangle \langle n|)$ denotes the reduced density matrix after evolving the corresponding input state. The process fidelity is then defined as [98]

$$\mathcal{F}_{\text{CZ}} = \left[\text{Tr} \left(\sqrt{\sqrt{\Phi} \Phi_{\text{true}} \sqrt{\Phi}} \right) \right]^2, \quad (14)$$

where Φ_{true} is the Choi matrix of the ideal CZ gate.

III. CONTROLLED-Z GATE

We now investigate how a CZ gate can be implemented using GAs coupled to a structured waveguide. The CZ gate applies a phase shift of π to the $|11\rangle$ state of a two-qubit system while leaving all other basis states unchanged. In our system, this operation can be achieved by coherently transferring the population of the $|11\rangle$ state to $|02\rangle$ or $|20\rangle$ and then bringing it back [100]; see Fig. 1(b). This process requires a resonant transition between these states. In our setup, we realize this resonance by setting $\omega_2 = \omega_1 + \alpha_1$, which enables a resonant coupling between $|11\rangle$ and $|20\rangle$.

To prevent radiative decay during the evolution, we require that transitions at both ω_1 and $\omega_1 + \alpha_1$ must be decoherence-free. Thus, implementing the CZ gate requires at least two decoherence-free frequencies within the photonic band. For a GA with coupling points x_j and coupling strengths g_j , the decoherence-free condition arises from destructive interference [29]:

$$\sum_j g_j \exp(ik_{\text{DF}} x_j) = 0, \quad (15)$$

where k_{DF} is a wave number that fulfills this equation.

A. Minimal two-point implementation

The most straightforward configuration that enables fulfilling all the above conditions involves two coupling points separated by Δx and uniform coupling strength, as shown in Fig. 2(a). In this case, Eq. (15) reduces to

$$1 + e^{ik_{\text{DF}} \Delta x} = 0 \quad \Rightarrow \quad k_{\text{DF}} = \frac{\pi + 2n\pi}{\Delta x}, \quad n \in \mathbb{N}. \quad (16)$$

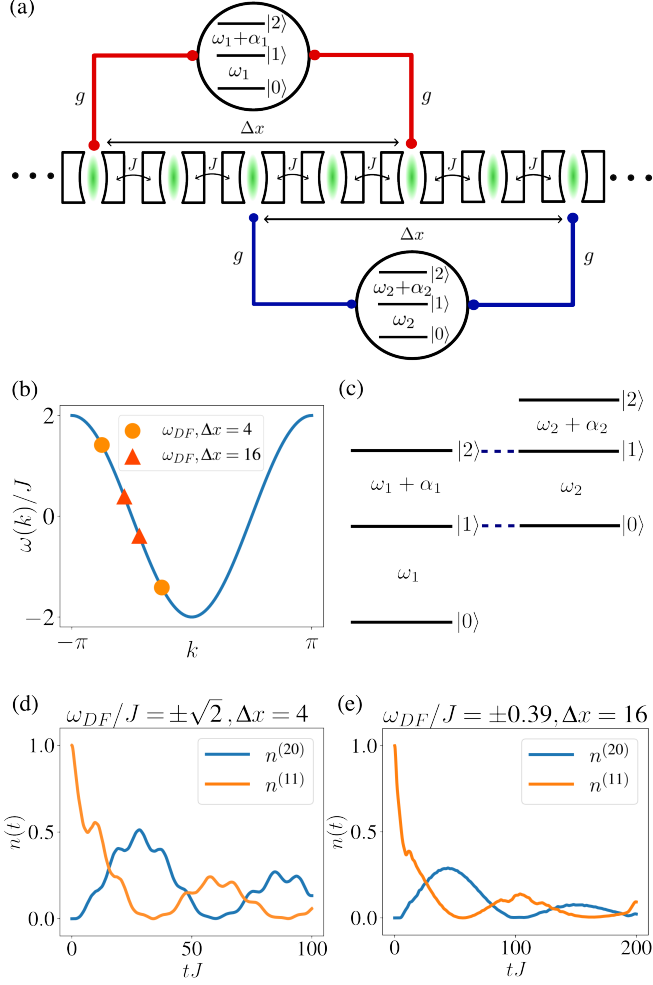


FIG. 2. Setup and results for performing a CZ gate between GAs with two coupling points each. (a) Schematic of the GA-based setup with two coupling points to perform a CZ gate. (b) Bath dispersion relation and the decoherence-free frequencies for $\Delta x = 4$ ($\omega_{\text{DF}}/J = \pm\sqrt{2}$) and $\Delta x = 16$ ($\omega_{\text{DF}}/J = \pm 0.39$) shown with circles and triangles, respectively. (c) Energy-level diagram of the two GAs for settings enabling the CZ gate. (d) Dynamics in the decoherence-free regime, with parameters $N = 100$, $g/J = 0.175$, $\omega_1/J = \sqrt{2}$, $\omega_2/J = -\sqrt{2}$, $\alpha_1/J = -2\sqrt{2}$, and $\alpha_2/J = -3$. (e) Same as in (d), but with increased separation $\Delta x = 16$ and parameters $\omega_1/J = 0.39$, $\omega_2/J = -0.39$, $\alpha_1/J = -0.78$, and $\alpha_2/J = -1$.

Using the dispersion relation from Eq. (5), we obtain the corresponding decoherence-free frequencies:

$$\omega_{\text{DF}} = -2J \cos\left(\frac{\pi + 2n\pi}{\Delta x}\right), \quad n \in \mathbb{N}. \quad (17)$$

To obtain two distinct DF frequencies within the band, we require $\Delta x \geq 3$. However, for $\Delta x = 3$, one of the DF frequencies is located at the band edge ($\omega_{\text{DF}} = 2J$), where strong non-Markovian effects dominate [55]. We therefore choose $\Delta x = 4$, yielding DF frequencies at $\omega_{\text{DF}} = \pm\sqrt{2}J$, as shown in Fig. 2(b).

To perform the CZ gate, the level spacings of the two GAs need to satisfy $\omega_1 + \alpha_1 = \omega_2$ [Fig. 2(c)] and that both ω_1 and ω_2 are decoherence-free. These conditions are satisfied for $\Delta x = 4$ with $\omega_1/J = \sqrt{2}$, $\omega_2/J = -\sqrt{2}$, and $\alpha_1/J = -2\sqrt{2}$. The parameter α_2 does not qualitatively influence the dynamics; we set $\alpha_2/J = -3$ to have it similar to the anharmonicity of atom 1.

The dynamics with the system configured thus and initialized in $|11\rangle_A$ is shown in Fig. 2(d). The populations of the $|20\rangle$ and $|11\rangle$ states are computed as

$$n^{(20)}(t) = \frac{1}{2} \langle \psi(t) | \sigma_1^{(2),+} \sigma_1^{(1),+} \sigma_1^{(1),-} \sigma_1^{(2),-} | \psi(t) \rangle, \quad (18)$$

$$n^{(11)}(t) = \langle \psi(t) | \sigma_2^{(1),+} \sigma_1^{(1),+} \sigma_1^{(1),-} \sigma_2^{(1),-} | \psi(t) \rangle, \quad (19)$$

where $|\psi(t)\rangle$ is the state at time t . Although this setup formally satisfies the DF condition, the DF frequencies lie far from the band center, leading to strong non-Markovian effects [55]. As a result, population decays rapidly, the DFI breaks down, and the two-point configuration fails to support a high-fidelity CZ gate.

A natural way to address this issue is to increase the separation Δx , which shifts the DF frequencies closer to the band center. For example, $\Delta x = 16$ yields $\omega_{\text{DF}}/J = \pm 0.39$, as shown in Fig. 2(b). However, as shown in Fig. 2(e), this strategy does not improve performance: the larger separation introduces a significant time delay for photons traveling between coupling points, enhancing non-Markovian effects leading to significant population loss into the waveguide.

B. Improvement with a three-point implementation

To overcome the limitations of the two-point configuration, we introduce a third coupling point placed in the middle between the original two, with a relative coupling strength ζ , as shown in Fig. 3(a). In this setup, the decoherence-free condition in Eq. (15) is modified to

$$1 + \zeta e^{ik_{\text{DF}}\Delta x} + e^{2ik_{\text{DF}}\Delta x} = 0. \quad (20)$$

The corresponding decoherence-free wavevectors are

$$k_{\text{DF}} = \frac{\arccos\left(-\frac{\zeta}{2}\right) + 2n\pi}{\Delta x}, \quad n \in \mathbb{N}, \quad (21)$$

with associated frequencies

$$\omega_{\text{DF}} = -2J \cos\left[\frac{\arccos\left(-\frac{\zeta}{2}\right) + 2n\pi}{\Delta x}\right], \quad n \in \mathbb{N}. \quad (22)$$

The dependence of ω_{DF} on ζ for $\Delta x = 2$ is shown in Fig. 3(b). As ζ increases, the DF frequencies shift progressively toward the center of the photonic band. At $\zeta = 2$, the two solutions merge at $\omega_{\text{DF}} = 0$.

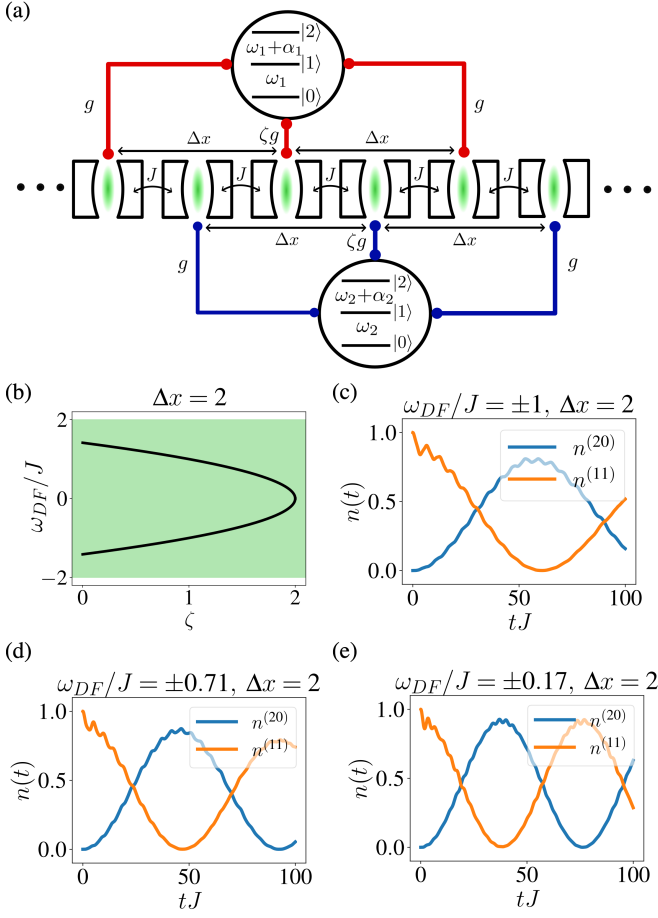


FIG. 3. Setup and results for performing a CZ gate between GAs with three coupling points each. (a) Schematic of the GA-based setup with three coupling points to perform a CZ gate, with $\Delta x = 2$ between adjacent coupling points. Compared to Fig. 2(a), a third, central coupling point with coupling strength ζg is added. This configuration yields two decoherence-free (DF) frequencies for $0 \leq \zeta < 2$. (b) Decoherence-free frequencies as a function of ζ , showing that the two frequencies merge at $\zeta = 2$ with the band of propagating frequencies between $[-2, 2]$ shown in light green. (c) Dynamics in the DFI regime for $N = 100$, $\Delta x = 2$, $g/J = 0.1$, and $\zeta = 1$, yielding DF frequencies $\omega_{DF}/J = \pm 1$. The frequencies and anharmonicities of the GAs are chosen to fit in the CZ-gate configuration: $\omega_1/J = 1$, $\omega_2/J = -0.98$, $\alpha_1/J = -2$, and $\alpha_2/J = -1.52$. (d) Same as (c), but with $\zeta = 1.5$, giving DF frequencies $\omega_{DF}/J = \pm 0.71$. Here, we take parameters $\omega_1/J = 0.71$, $\omega_2/J = -0.69$, $\alpha_1/J = -1.42$, and $\alpha_2/J = -1.31$. (e) Same as (c) and (d), but with $\zeta = 1.97$, resulting in DF frequencies $\omega_{DF}/J = \pm 0.17$. Here, we take parameters $\omega_1/J = 0.17$, $\omega_2/J = -0.17$, $\alpha_1/J = -0.34$, and $\alpha_2/J = -0.67$.

The dynamics for this configuration are illustrated in Fig. 3(c)–(e) for three successively increasing values of ζ matched to the decoherence-free conditions required for the CZ gate. As ζ increases, the quality of the DFI improves: after a full cycle, a larger fraction of the population returns to $|11\rangle$, which is essential for high-fidelity

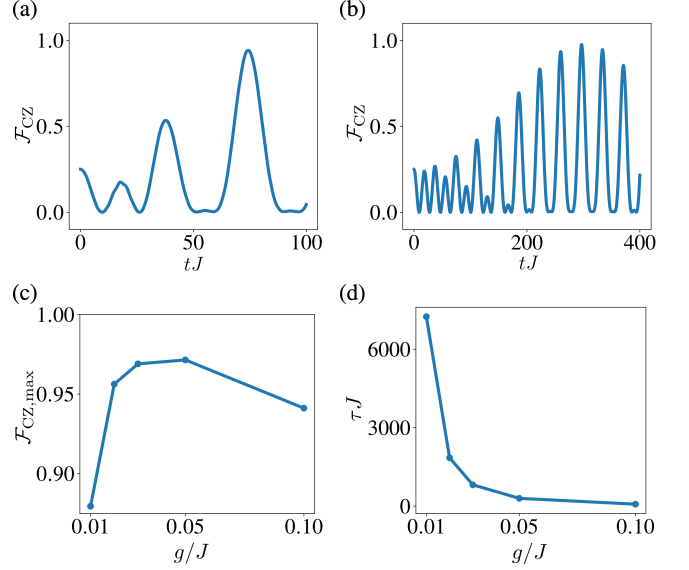


FIG. 4. Process fidelity \mathcal{F}_{CZ} of CZ gates performed with the setup in Fig. 3(a). (a) Process fidelity as a function of time t for the same parameters as in Fig. 3(e). (b) Same as (a), but with a smaller $g = 0.05J$. (c) The best process fidelity of CZ gates, $\mathcal{F}_{CZ,max}$, for different values of g , considering realistic qubit and cavity decay rates of $\Gamma_q = 1.6 \cdot 10^{-5} J$ and $\Gamma_c = 8 \cdot 10^{-5} J$. (d) The gate time τ required for the best CZ gate in (c).

CZ gate operation. This enhancement stems from the suppression of non-Markovian effects, since the relevant DF frequencies are brought closer to the band center.

We note that the $|1\rangle \rightarrow |0\rangle$ transition of atom 2 is also off-resonantly coupled to the $|1\rangle \rightarrow |0\rangle$ transition in atom 1. As a consequence, to obtain a coherent population exchange between the atoms, ω_2 needs to deviate slightly from $\omega_1 + \alpha_1$ to take into account the Lamb shift [101] resulting from this coupling; hence the parameter choices in Fig. 3(c)–(d). We also note that the gate dynamics become faster for larger ζ , as a consequence of the increased effective coupling between the atom and the waveguide.

C. Gate fidelity

Having analyzed the improved setup for performing a CZ gate with GAs in Fig. 3, we now compute the corresponding gate fidelity, as described in Section II C. The process fidelity \mathcal{F}_{CZ} during the time evolution is shown in Fig. 4(a) for the parameters from Fig. 3(a). A maximum process fidelity of 94.2% is achieved at $tJ = 74.0$, corresponding to the time at which the population is transferred from $|11\rangle$ to $|20\rangle$ and back. The corresponding average gate fidelity is $F_{CZ} \approx 95.4\%$. For ideal qubits and cavities, the fidelity can be further improved by reducing the coupling strength g . For example, choosing $g = 0.05J$ increases the process fidelity to $\mathcal{F}_{CZ} \approx 97.6\%$, reached at $tJ = 296.8$ [Fig. 4(b)].

In realistic scenarios, where qubits and cavities exhibit intrinsic decay, a comprehensive optimization of the coupling strength g would require solving the full master equation. This significantly increases the computational cost, as the Liouvillian superoperator scales with the square of the Hilbert-space dimension [102]. To make the problem tractable, we instead analyze decay effects using the following effective non-Hermitian Hamiltonian, obtained by neglecting quantum jumps and collective decay processes:

$$H_{\text{eff}} = H - \frac{i\Gamma_q}{2} \sum_{m=1}^2 \left[\sigma_m^{(2),+} \sigma_m^{(2),-} + \sigma_m^{(1),+} \sigma_m^{(1),-} \right] - \frac{i\Gamma_c}{2} \sum_{n=1}^N a_n^\dagger a_n. \quad (23)$$

Here, H denotes the ideal system Hamiltonian defined in Eq. (1) and $\Gamma_{q(c)}$ is the qubit (cavity) decay rate, assumed identical for all qubits (cavities). The higher decay rate of the $|2\rangle$ level compared to $|1\rangle$ is incorporated through the definition of $\sigma_m^{(2),\pm}$ in Eq. (3).

We now evaluate the CZ gate fidelity for experimentally relevant parameters in superconducting circuits, where GAs have already been demonstrated [31, 36, 39, 41, 72]. In particular, transmon qubits [103] coupled to microwave resonators provide a promising platform for implementing our proposal. In state-of-the-art devices, the transmon anharmonicity can be as low as $-\alpha/2\pi \approx 50$ MHz [104, 105], while the inter-cavity coupling between microwave resonators can reach $J/2\pi \approx 200$ MHz [106], yielding a ratio $-\alpha/J \approx 1/4$. Our choice of $-\alpha/J = 1/3$ in Fig. 3(e) is therefore conservative. Furthermore, a coupling strength of $g/2\pi = 0.05J/2\pi \approx 10$ MHz is well within reach of current superconducting circuit technology [31, 41]. The required strength of the central coupling point with $0 \leq \zeta < 2$ is modest and experimentally accessible [31, 41]. A conservative estimation of typical decay rates for transmons and microwave resonators are $\Gamma_q = 0.02$ MHz and $\Gamma_c = 0.1$ MHz, respectively (for resonators operating at 5 GHz; even lower rates are achievable at smaller resonator frequencies) [107–115]. For $J/2\pi = 200$ MHz, these values correspond to $\Gamma_q = 1.6 \times 10^{-5}J$ and $\Gamma_c = 8 \times 10^{-5}J$, which we adopt in our analysis.

For different values of g , the optimal process fidelity $\mathcal{F}_{\text{CZ,max}}$ and the corresponding gate time τ are shown in Fig. 4(c)–(d). For large g , the gate time τ is short, and decoherence from qubits and cavities does not constitute the primary limitation to fidelity [116, 117]. In contrast, for small g , the increased gate time makes intrinsic decay the dominant source of infidelity. Consequently, the optimal performance is obtained at $g = 0.05J$ with gate time $\tau = 297/J \approx 236$ ns, yielding a process fidelity of $\mathcal{F}_{\text{CZ}} \approx 97.1\%$, corresponding to an average gate fidelity of $F_{\text{CZ}} \approx 97.7\%$.

IV. CONCLUSION

We have demonstrated how a controlled-Z (CZ) gate can be implemented using giant atoms (GAs) coupled to a structured waveguide. Starting from a minimal two-point coupling configuration, we showed that although the required decoherence-free interaction (DFI) can be realized, strong non-Markovian effects significantly limit the achievable gate fidelity. To address this limitation, we proposed an extended configuration that includes a third, intermediate coupling point. This modification shifts the decoherence-free frequencies closer to the center of the photonic band, thereby mitigating non-Markovian effects. With this design, we can achieve CZ gates with fidelities up to 97.7% when including realistic imperfections like typical resonator and transmon decay rates; remaining non-Markovian effects from spacing between coupling points also contribute to reducing the gate fidelity.

Beyond the specific case of the CZ gate, our results establish a general strategy for engineering multi-photon processes in structured waveguide QED by tailoring interference conditions through multi-point coupling. This approach opens new possibilities for realizing other entangling operations, exploiting strongly correlated photonic dynamics, and extending gate protocols to larger networks of GAs. Moreover, the protocol is compatible with state-of-the-art superconducting circuits, where transmon coherence times are orders of magnitude longer than the gate duration, suggesting that experimental realization is within reach.

Looking ahead, our findings point toward several promising directions. One is the integration of multiple GAs in extended resonator arrays, enabling scalable architectures for quantum computation and simulation, such as passive-leakage reset for high-fidelity gates [118]. Another is the exploration of richer structured environments, such as topological or chiral waveguides, where decoherence-free conditions could be further stabilized, or new types of protected interactions could emerge. More broadly, the interplay between photon-photon interactions [119], engineered dispersion, and non-Markovian dynamics in these systems defines a fertile platform for advancing fundamental studies of open quantum systems.

ACKNOWLEDGMENTS

All code used in this work are open access via GitHub: <https://github.com/Q-WAVES/GiantAtoms/>. A.S. acknowledges fruitful discussions with Simon Pettersson Fors. G.C. is supported by European Union's Horizon Europe programme HORIZON-MSCA-2023-PF-01-01 via the project 101146565 (SING-ATOM). W.R., A.S., and A.F.K. acknowledge support from the Swedish Foundation for Strategic Research (grant number FFL21-0279). A.F.K. is also supported by the Swedish Founda-

tion for Strategic Research (grant number FUS21-0063), the Horizon Europe programme HORIZON-CL4-2022-QUANTUM-01-SGA via the project 101113946 OpenSu-

perQPlus100, and from the Knut and Alice Wallenberg Foundation through the Wallenberg Centre for Quantum Technology (WACQT).

-
- [1] I. M. Georgescu, S. Ashhab, and F. Nori, Quantum simulation, *Reviews of Modern Physics* **86**, 153 (2014).
- [2] E. Altman *et al.*, Quantum Simulators: Architectures and Opportunities, *PRX Quantum* **2**, 017003 (2021).
- [3] B. Fauseweh, Quantum many-body simulations on digital quantum computers: State-of-the-art and future challenges, *Nature Communications* **15**, 2123 (2024).
- [4] K. Wintersperger, F. Dommert, T. Ehmer, A. Hourasanov, J. Klepsch, W. Mauerer, G. Reuber, T. Strohm, M. Yin, and S. Luber, Neutral atom quantum computing hardware: performance and end-user perspective, *EPJ Quantum Technology* **10**, 32 (2023).
- [5] T. Strohm, K. Wintersperger, F. Dommert, D. Basilewitsch, G. Reuber, A. Hourasanov, T. Ehmer, D. Vodola, and S. Luber, Ion-Based Quantum Computing Hardware: Performance and End-User Perspective (2024), [arXiv:2405.11450](https://arxiv.org/abs/2405.11450).
- [6] S. A. Caldwell, N. Didier, C. A. Ryan, E. A. Sete, A. Hudson, P. Karalekas, R. Manenti, M. P. da Silva, R. Sinclair, E. Acala, N. Alidoust, J. Angeles, A. Bestwick, M. Block, B. Bloom, A. Bradley, C. Bui, L. Capelluto, R. Chilcott, J. Cordova, G. Crossman, M. Curtis, S. Deshpande, T. E. Bouayadi, D. Girshovich, S. Hong, K. Kuang, M. Lenihan, T. Manning, A. Marchenkov, J. Marshall, R. Maydra, Y. Mohan, W. O'Brien, C. Osborn, J. Otterbach, A. Papageorge, J.-P. Paquette, M. Pelstring, A. Polloreno, G. Prawiroatmodjo, V. Rawat, M. Reagor, R. Renzas, N. Rubin, D. Russell, M. Rust, D. Scarabelli, M. Scheer, M. Selvanayagam, R. Smith, A. Staley, M. Suska, N. Tezak, D. C. Thompson, T.-W. To, M. Vahidpour, N. Vodrahalli, T. Whyland, K. Yadav, W. Zeng, and C. Rigetti, Parametrically Activated Entangling Gates Using Transmon Qubits, *Physical Review Applied* **10**, 034050 (2018).
- [7] R. Barends, C. M. Quintana, A. G. Petukhov, Y. Chen, D. Kafri, K. Kechedzhi, R. Collins, O. Naaman, S. Boixo, F. Arute, K. Arya, D. Buell, B. Burkett, Z. Chen, B. Chiaro, A. Dunsworth, B. Foxen, A. Fowler, C. Gidney, M. Giustina, R. Graff, T. Huang, E. Jeffrey, J. Kelly, P. V. Klimov, F. Kostritsa, D. Landhuis, E. Lucero, M. McEwen, A. Megrant, X. Mi, J. Mutus, M. Neeley, C. Neill, E. Ostby, P. Roushan, D. Sank, K. J. Satzinger, A. Vainsencher, T. White, J. Yao, P. Yeh, A. Zalcman, H. Neven, V. N. Smelyanskiy, and J. M. Martinis, Diabatic Gates for Frequency-Tunable Superconducting Qubits, *Physical Review Letters* **123**, 210501 (2019).
- [8] A. Noguchi, A. Osada, S. Masuda, S. Kono, K. Heya, S. P. Wolski, H. Takahashi, T. Sugiyama, D. Lachance-Quirion, and Y. Nakamura, Fast parametric two-qubit gates with suppressed residual interaction using the second-order nonlinearity of a cubic transmon, *Physical Review A* **102**, 062408 (2020).
- [9] D. M. Abrams, N. Didier, B. R. Johnson, M. P. d. Silva, and C. A. Ryan, Implementation of XY entangling gates with a single calibrated pulse, *Nature Electronics* **3**, 744 (2020).
- [10] M. Ganzhorn, G. Salis, D. J. Egger, A. Fuhrer, M. Mergenthaler, C. Müller, P. Müller, S. Paredes, M. Pechal, M. Werninghaus, and S. Filipp, Benchmarking the noise sensitivity of different parametric two-qubit gates in a single superconducting quantum computing platform, *Physical Review Research* **2**, 033447 (2020).
- [11] N. Lacroix, C. Hellings, C. K. Andersen, A. Di Paolo, A. Remm, S. Lazar, S. Krinner, G. J. Norris, M. Gabureac, J. Heinsoo, A. Blais, C. Eichler, and A. Wallraff, Improving the Performance of Deep Quantum Optimization Algorithms with Continuous Gate Sets, *PRX Quantum* **1**, 110304 (2020).
- [12] E. A. Sete, N. Didier, A. Q. Chen, S. Kulshreshtha, R. Manenti, and S. Poletto, Parametric-Resonance Entangling Gates with a Tunable Coupler, *Physical Review Applied* **16**, 024050 (2021).
- [13] E. A. Sete, N. Didier, A. Q. Chen, S. Kulshreshtha, R. Manenti, and S. Poletto, Parametric-Resonance Entangling Gates with a Tunable Coupler, *Physical Review Applied* **16**, 024050 (2021).
- [14] Y. Sung, L. Ding, J. Braumüller, A. Vepsäläinen, B. Kannan, M. Kjaergaard, A. Greene, G. O. Samach, C. McNally, D. Kim, A. Melville, B. M. Niedzielski, M. E. Schwartz, J. L. Yoder, T. P. Orlando, S. Gustavsson, and W. D. Oliver, Realization of High-Fidelity CZ and ZZ-Free iSWAP Gates with a Tunable Coupler, *Physical Review X* **11**, 021058 (2021).
- [15] Rigetti QCS, *Aspen-M-3 Quantum Processor* (2023).
- [16] H. Zhang, C. Ding, D. Weiss, Z. Huang, Y. Ma, C. Guinn, S. Sussman, S. P. Chitta, D. Chen, A. A. Houck, J. Koch, and D. I. Schuster, Tunable Inductive Coupler for High-Fidelity Gates Between Fluxonium Qubits, *PRX Quantum* **5**, 020326 (2024).
- [17] Z. Chen, W. Liu, Y. Ma, W. Sun, R. Wang, H. Wang, H. Xu, G. Xue, H. Yan, Z. Yang, J. Ding, Y. Gao, F. Li, Y. Zhang, Z. Zhang, Y. Jin, H. Yu, J. Chen, and F. Yan, Efficient implementation of arbitrary two-qubit gates via unified control, *Nature Physics* **21**, 1489 (2025).
- [18] T.-M. Li, J.-C. Zhang, B.-J. Chen, K. Huang, H.-T. Liu, Y.-X. Xiao, C.-L. Deng, G.-H. Liang, C.-T. Chen, Y. Liu, H. Li, Z.-T. Bao, K. Zhao, Y. Xu, L. Li, Y. He, Z.-H. Liu, Y.-H. Yu, S.-Y. Zhou, Y.-J. Liu, X. Song, D. Zheng, Z. Xiang, Y.-H. Shi, K. Xu, and H. Fan, High-precision pulse calibration of tunable couplers for high-fidelity two-qubit gates in superconducting quantum processors, *Physical Review Applied* **23**, 024059 (2025).
- [19] C. Križan, J. Biznárová, L. Chen, E. Hogedal, A. Osman, C. W. Warren, S. Kosen, H.-x. Li, T. Abad, A. Aggarwal, M. Caputo, J. Fernández-Pendás, A. Gaikwad, L. Grönberg, A. Nylander, R. Rehammar, M. Rommel, O. I. Yuzepovich, A. Frisk Kockum, J. Govenius, G. Tancredi, and J. Bylander, Quantum SWAP gate realized with CZ and iSWAP gates in a superconducting

- architecture, *New Journal of Physics* **27**, 074507 (2025).
- [20] H.-T. Liu, B.-J. Chen, J.-C. Zhang, Y.-X. Xiao, T.-M. Li, K. Huang, Z. Wang, H. Li, K. Zhao, Y. Xu, C.-L. Deng, G.-H. Liang, Z.-H. Liu, S.-Y. Zhou, C.-P. Fang, X. Song, Z. Xiang, D. Zheng, Y.-H. Shi, K. Xu, and H. Fan, Direct Implementation of High-Fidelity Three-Qubit Gates for Superconducting Processor with Tunable Couplers, *Physical Review Letters* **135**, 050602 (2025).
- [21] K. X. Wei, E. Magesan, I. Lauer, S. Srinivasan, D. F. Bogorin, S. Carnevale, G. A. Keefe, Y. Kim, D. Klaus, W. Landers, N. Sundaresan, C. Wang, E. J. Zhang, M. Steffen, O. E. Dial, D. C. McKay, and A. Kandala, Hamiltonian Engineering with Multicolor Drives for Fast Entangling Gates and Quantum Crosstalk Cancellation, *Physical Review Letters* **129**, 060501 (2022).
- [22] L. B. Nguyen, Y. Kim, A. Hashim, N. Goss, B. Marinelli, B. Bhandari, D. Das, R. K. Naik, J. M. Kreikebaum, A. N. Jordan, D. I. Santiago, and I. Siddiqi, Programmable Heisenberg interactions between Floquet qubits, *Nature Physics* **20**, 240 (2024).
- [23] H. Zhang, C. Ding, D. Weiss, Z. Huang, Y. Ma, C. Guinn, S. Sussman, S. P. Chitta, D. Chen, A. A. Houck, J. Koch, and D. I. Schuster, Tunable Inductive Coupler for High-Fidelity Gates Between Fluxonium Qubits, *PRX Quantum* **5**, 020326 (2024).
- [24] S. J. Evered, D. Bluvstein, M. Kalinowski, S. Ebadi, T. Manovitz, H. Zhou, S. H. Li, A. A. Geim, T. T. Wang, N. Maskara, H. Levine, G. Semeghini, M. Greiner, V. Vuletić, and M. D. Lukin, High-fidelity parallel entangling gates on a neutral-atom quantum computer, *Nature* **622**, 268 (2023).
- [25] B. Foxen, C. Neill, A. Dunsworth, P. Roushan, B. Chiaro, A. Megrant, J. Kelly, Z. Chen, K. Satzinger, R. Barends, F. Arute, K. Arya, R. Babbush, D. Bacon, J. C. Bardin, S. Boixo, D. Buell, B. Burkett, Y. Chen, R. Collins, E. Farhi, A. Fowler, C. Gidney, M. Giustina, R. Graff, M. Harrigan, T. Huang, S. V. Isakov, E. Jeffrey, Z. Jiang, D. Kafri, K. Kechedzhi, P. Klimov, A. Korotkov, F. Kostritsa, D. Landhuis, E. Lucero, J. McClean, M. McEwen, X. Mi, M. Mohseni, J. Y. Mutus, O. Naaman, M. Neeley, M. Niu, A. Petukhov, C. Quintana, N. Rubin, D. Sank, V. Smelyanskiy, A. Vainsencher, T. C. White, Z. Yao, P. Yeh, A. Zalcman, H. Neven, and J. M. Martinis, Demonstrating a Continuous Set of Two-Qubit Gates for Near-Term Quantum Algorithms, *Physical Review Letters* **125**, 120504 (2020).
- [26] K. X. Wei, I. Lauer, E. Pritchett, W. Shanks, D. C. McKay, and A. Javadi-Abhari, Native Two-Qubit Gates in Fixed-Coupling, Fixed-Frequency Transmons Beyond Cross-Resonance Interaction, *PRX Quantum* **5**, 020338 (2024).
- [27] A. F. Kockum, Quantum Optics with Giant Atoms - the First Five Years, in *International Symposium on Mathematics, Quantum Theory, and Cryptography (Mathematics for Industry, vol 33)* (Springer, 2021) pp. 125–146.
- [28] M. V. Gustafsson, T. Aref, A. F. Kockum, M. K. Ekström, G. Johansson, and P. Delsing, Propagating phonons coupled to an artificial atom, *Science* **346**, 207 (2014).
- [29] A. Frisk Kockum, P. Delsing, and G. Johansson, Designing frequency-dependent relaxation rates and Lamb shifts for a giant artificial atom, *Physical Review A* **90**, 013837 (2014).
- [30] A. F. Kockum, G. Johansson, and F. Nori, Decoherence-Free Interaction between Giant Atoms in Waveguide Quantum Electrodynamics, *Physical Review Letters* **120**, 140404 (2018).
- [31] B. Kannan, M. J. Ruckriegel, D. L. Campbell, A. Frisk Kockum, J. Braumüller, D. K. Kim, M. Kjaergaard, P. Krantz, A. Melville, B. M. Niedzielski, A. Vepsäläinen, R. Winik, J. L. Yoder, F. Nori, T. P. Orlando, S. Gustavsson, and W. D. Oliver, Waveguide quantum electrodynamics with superconducting artificial giant atoms, *Nature* **583**, 775 (2020).
- [32] G. Chen and A. Frisk Kockum, Simulating open quantum systems with giant atoms, *Quantum Science and Technology* **10**, 025028 (2025).
- [33] C. L. Yang and W. Z. Jia, Simulating and probing many-body quantum states in waveguide-QED systems with giant atoms, *Physical Review A* **111**, 023712 (2025).
- [34] G. Chen and A. F. Kockum, Scalable quantum simulator with an extended gate set in giant atoms (2025), [arXiv:2503.04537](https://arxiv.org/abs/2503.04537).
- [35] G. Chen and A. F. Kockum, Efficient three-qubit gates with giant atoms (2025), [arXiv:2510.04545](https://arxiv.org/abs/2510.04545).
- [36] A. M. Vadiraj, A. Ask, T. G. McConkey, I. Nsanzeza, C. W. S. Chang, A. F. Kockum, and C. M. Wilson, Engineering the level structure of a giant artificial atom in waveguide quantum electrodynamics, *Physical Review A* **103**, 023710 (2021).
- [37] Z. Q. Wang, Y. P. Wang, J. Yao, R. C. Shen, W. J. Wu, J. Qian, J. Li, S. Y. Zhu, and J. Q. You, Giant spin ensembles in waveguide magnonics, *Nature Communications* **13**, 7580 (2022).
- [38] Y.-T. Chen, L. Du, L. Guo, Z. Wang, Y. Zhang, Y. Li, and J.-H. Wu, Nonreciprocal and chiral single-photon scattering for giant atoms, *Communications Physics* **5**, 215 (2022).
- [39] C. Joshi, F. Yang, and M. Mirhosseini, Resonance Fluorescence of a Chiral Artificial Atom, *Physical Review X* **13**, 021039 (2023).
- [40] X. Wang, H.-B. Zhu, T. Liu, and F. Nori, Realizing quantum optics in structured environments with giant atoms, *Physical Review Research* **6**, 013279 (2024).
- [41] V. Jouanny, L. Peyruchat, M. Scigliuzzo, A. Mercurio, E. Di Benedetto, D. De Bernardis, D. Sbroggiò, S. Frasca, V. Savona, F. Ciccarello, and P. Scarlino, Superstrong Dynamics and Chiral Emission of a Giant Atom in a Structured Bath (2025), [arXiv:2509.01579](https://arxiv.org/abs/2509.01579).
- [42] L. Guo, A. L. Grimsmo, A. F. Kockum, M. Pletyukhov, and G. Johansson, Giant acoustic atom: A single quantum system with a deterministic time delay, *Physical Review A* **95**, 053821 (2017).
- [43] A. González-Tudela, C. S. Muñoz, and J. I. Cirac, Engineering and Harnessing Giant Atoms in High-Dimensional Baths: A Proposal for Implementation with Cold Atoms, *Physical Review Letters* **122**, 203603 (2019).
- [44] L. Guo, A. F. Kockum, F. Marquardt, and G. Johansson, Oscillating bound states for a giant atom, *Physical Review Research* **2**, 043014 (2020).
- [45] P. O. Guimond, B. Vermersch, M. L. Juan, A. Sharafiev, G. Kirchmair, and P. Zoller, A unidirectional on-chip photonic interface for superconducting circuits, *npj Quantum Information* **6**, 32 (2020).

- [46] A. Ask, Y.-L. L. Fang, and A. F. Kockum, Synthesizing electromagnetically induced transparency without a control field in waveguide QED using small and giant atoms (2020), [arXiv:2011.15077](#).
- [47] D. Cilluffo, A. Carollo, S. Lorenzo, J. A. Gross, G. M. Palma, and F. Ciccarello, Collisional picture of quantum optics with giant emitters, *Physical Review Research* **2**, 043070 (2020).
- [48] X. Wang, T. Liu, A. F. Kockum, H.-R. Li, and F. Nori, Tunable Chiral Bound States with Giant Atoms, *Physical Review Letters* **126**, 043602 (2021).
- [49] L. Du and Y. Li, Single-photon frequency conversion via a giant Λ -type atom, *Physical Review A* **104**, 023712 (2021).
- [50] A. Soro and A. F. Kockum, Chiral quantum optics with giant atoms, *Physical Review A* **105**, 023712 (2022).
- [51] X. Wang and H.-r. Li, Chiral quantum network with giant atoms, *Quantum Science and Technology* **7**, 035007 (2022).
- [52] L. Du, Y. Zhang, J. H. Wu, A. F. Kockum, and Y. Li, Giant Atoms in a Synthetic Frequency Dimension, *Physical Review Letters* **128**, 223602 (2022).
- [53] L. Du, Y.-T. Chen, Y. Zhang, and Y. Li, Giant atoms with time-dependent couplings, *Physical Review Research* **4**, 023198 (2022).
- [54] S. Terradas-Briansó, C. A. González-Gutiérrez, F. Nori, L. Martín-Moreno, and D. Zueco, Ultrastrong waveguide QED with giant atoms, *Physical Review A* **106**, 063717 (2022).
- [55] A. Soro, C. S. Muñoz, and A. F. Kockum, Interaction between giant atoms in a one-dimensional structured environment, *Physical Review A* **107**, 013710 (2023).
- [56] L. Du, L. Guo, Y. Zhang, and A. F. Kockum, Giant emitters in a structured bath with non-Hermitian skin effect, *Physical Review Research* **5**, L042040 (2023).
- [57] E. Raaholt Ingelsten, A. F. Kockum, and A. Soro, Avoiding decoherence with giant atoms in a two-dimensional structured environment, *Physical Review Research* **6**, 043222 (2024).
- [58] L. Leonforte, X. Sun, D. Valenti, B. Spagnolo, F. Illuminati, A. Carollo, and F. Ciccarello, Quantum optics with giant atoms in a structured photonic bath, *Quantum Science and Technology* **10**, 015057 (2025).
- [59] F. Roccati and D. Cilluffo, Controlling Markovianity with Chiral Giant Atoms, *Physical Review Letters* **133**, 063603 (2024).
- [60] R.-Y. Gong, Z.-Y. He, C.-H. Yu, G.-F. Zhang, F. Nori, and Z.-L. Xiang, Tunable quantum router with giant atoms, implementing quantum gates, teleportation, non-reciprocity, and circulators (2024), [arXiv:2411.19307](#).
- [61] L. Du and A. F. Kockum, Unconventional and robust light-matter interactions based on the non-Hermitian skin effect, *Physical Review Research* **7**, 013140 (2025).
- [62] L. Du, X. Wang, A. F. Kockum, and J. Splettstoesser, Dressed Interference in Giant Superatoms: Entanglement Generation and Transfer, *Physical Review Letters* **135**, 223601 (2025).
- [63] T. Levy-Yeyati, T. Ramos, and A. González-Tudela, Engineering giant transmon molecules as mediators of conditional two-photon gates (2025), [arXiv:2507.05377](#).
- [64] J.-Q. Li, A. F. Kockum, and X. Wang, Generating spatially separated correlated multiphoton states in nonlinear waveguide quantum electrodynamics (2025), [arXiv:2511.14281](#).
- [65] W. Rieck, A. F. Kockum, and G. Chen, Doublon bound states in the continuum through giant atoms (2025), [arXiv:2511.18212](#).
- [66] R. Manenti, A. F. Kockum, A. Patterson, T. Behrle, J. Rahamim, G. Tancredi, F. Nori, and P. J. Leek, Circuit quantum acoustodynamics with surface acoustic waves, *Nature Communications* **8**, 975 (2017).
- [67] K. J. Satzinger, Y. P. Zhong, H.-S. Chang, G. A. Peairs, A. Bienfait, M.-H. Chou, A. Y. Cleland, C. R. Conner, É. Dumur, J. Grebel, I. Gutierrez, B. H. November, R. G. Povey, S. J. Whiteley, D. D. Awschalom, D. I. Schuster, and A. N. Cleland, Quantum control of surface acoustic-wave phonons, *Nature* **563**, 661 (2018).
- [68] A. Bienfait, K. J. Satzinger, Y. P. Zhong, H.-S. Chang, M.-H. Chou, C. R. Conner, É. Dumur, J. Grebel, G. A. Peairs, R. G. Povey, and A. N. Cleland, Phonon-mediated quantum state transfer and remote qubit entanglement, *Science* **364**, 368 (2019).
- [69] G. Andersson, B. Suri, L. Guo, T. Aref, and P. Delsing, Non-exponential decay of a giant artificial atom, *Nature Physics* **15**, 1123 (2019).
- [70] A. Bienfait, Y. P. Zhong, H.-S. Chang, M.-H. Chou, C. R. Conner, É. Dumur, J. Grebel, G. A. Peairs, R. G. Povey, K. J. Satzinger, and A. N. Cleland, Quantum Erasure Using Entangled Surface Acoustic Phonons, *Physical Review X* **10**, 021055 (2020).
- [71] G. Andersson, M. K. Ekström, and P. Delsing, Electromagnetically Induced Acoustic Transparency with a Superconducting Circuit, *Physical Review Letters* **124**, 240402 (2020).
- [72] J. Hu, D. Li, Y. Qie, Z. Yin, A. F. Kockum, F. Nori, and S. An, Engineering the Environment of a Superconducting Qubit with an Artificial Giant Atom (2024), [arXiv:2410.15377](#).
- [73] A. Almanakly, B. Yankelevich, M. Hays, B. Kannan, R. Assouly, A. Greene, M. Gingras, B. M. Niedzielski, H. Stickler, M. E. Schwartz, K. Serniak, J. Í.-j. Wang, T. P. Orlando, S. Gustavsson, J. A. Grover, and W. D. Oliver, Deterministic remote entanglement using a chiral quantum interconnect, *Nature Physics* **21**, 825 (2025).
- [74] L. Xiao, B. Zhang, Y. Zeng, X. Pan, J.-Q. Wang, Z. Hua, H. Huang, Y. Xu, G. Xue, H. Yu, X.-B. Xu, W. Wang, C.-L. Zou, and L. Sun, Giant-atom quantum acoustodynamics in hybrid superconducting-phononic integrated circuits (2025), [arXiv:2512.16582](#).
- [75] G. Calajó, F. Ciccarello, D. Chang, and P. Rabl, Atom-field dressed states in slow-light waveguide QED, *Physical Review A* **93**, 033833 (2016).
- [76] D. E. Chang, J. S. Douglas, A. González-Tudela, C.-L. Hung, and H. J. Kimble, Colloquium: Quantum matter built from nanoscopic lattices of atoms and photons, *Reviews of Modern Physics* **90**, 031002 (2018).
- [77] A. González-Tudela and J. I. Cirac, Quantum Emitters in Two-Dimensional Structured Reservoirs in the Nonperturbative Regime, *Physical Review Letters* **119**, 143602 (2017).
- [78] M. Scigliuzzo, G. Calajò, F. Ciccarello, D. Perez Lozano, A. Bengtsson, P. Scarlino, A. Wallraff, D. Chang, P. Delsing, and S. Gasparinetti, Controlling Atom-Photon Bound States in an Array of Josephson-Junction Resonators, *Physical Review X* **12**, 031036 (2022).

- [79] V. Jouanny, S. Frasca, V. J. Weibel, I. Peyruchat, M. Scigliuzzo, F. Oppliger, F. De Palma, D. Sbroggiò, G. Beaulieu, O. Zilberberg, and P. Scarlino, High kinetic inductance cavity arrays for compact band engineering and topology-based disorder meters, *Nature Communications* **16**, 3396 (2025).
- [80] C. Castillo-Moreno, K. R. Amin, I. Strandberg, M. Kervinen, A. Osman, and S. Gasparinetti, Dynamical Excitation Control and Multimode Emission of an Atom-Photon Bound State, *Physical Review Letters* **134**, 133601 (2025).
- [81] Y. Liu and A. A. Houck, Quantum electrodynamics near a photonic bandgap, *Nature Physics* **13**, 48 (2016).
- [82] N. M. Sundaresan, R. Lundgren, G. Zhu, A. V. Gorshkov, and A. A. Houck, Interacting Qubit-Photon Bound States with Superconducting Circuits, *Physical Review X* **9**, 011021 (2019).
- [83] P. M. Harrington, M. Naghiloo, D. Tan, and K. W. Murch, Bath engineering of a fluorescing artificial atom with a photonic crystal, *Physical Review A* **99**, 052126 (2019).
- [84] K. H. Lim, W.-K. Mok, and L.-C. Kwek, Oscillating bound states in non-Markovian photonic lattices, *Physical Review A* **107**, 023716 (2023).
- [85] S. Longhi, Photonic simulation of giant atom decay, *Optics Letters* **45**, 3017 (2020).
- [86] W. Zhao and Z. Wang, Single-photon scattering and bound states in an atom-waveguide system with two or multiple coupling points, *Physical Review A* **101**, 053855 (2020).
- [87] S. Longhi, Rabi oscillations of bound states in the continuum, *Optics Letters* **46**, 2091 (2021).
- [88] H. Yu, Z. Wang, and J.-H. Wu, Entanglement preparation and nonreciprocal excitation evolution in giant atoms by controllable dissipation and coupling, *Physical Review A* **104**, 013720 (2021).
- [89] C. Vega, M. Bello, D. Porras, and A. González-Tudela, Qubit-photon bound states in topological waveguides with long-range hoppings, *Physical Review A* **104**, 053522 (2021).
- [90] H. Xiao, L. Wang, Z. Li, X. Chen, and L. Yuan, Bound state in a giant atom-modulated resonators system, *npj Quantum Information* **8**, 80 (2022).
- [91] W. Cheng, Z. Wang, and Y. X. Liu, Topology and retardation effect of a giant atom in a topological waveguide, *Physical Review A* **106**, 033522 (2022).
- [92] X. Zhang, W. Cheng, Z. Gong, T. Zheng, and Z. Wang, Superconducting giant atom waveguide QED: Quantum Zeno and anti-Zeno effects in ultrastrong coupling regime (2022), [arXiv:2205.03674](https://arxiv.org/abs/2205.03674).
- [93] L. Du, L. Guo, Y. Zhang, and A. F. Kockum, Giant emitters in a structured bath with non-Hermitian skin effect, *Physical Review Research* **5**, L042040 (2023).
- [94] L. Du, Y.-T. Chen, Y. Zhang, Y. Li, and J.-H. Wu, Decay dynamics of a giant atom in a structured bath with broken time-reversal symmetry, *Quantum Science and Technology* **8**, 045010 (2023).
- [95] R. Bag and D. Roy, Quantum light-matter interactions in structured waveguides, *Physical Review A* **108**, 053717 (2023).
- [96] W. Z. Jia and M. T. Yu, Atom-photon dressed states in a waveguide-QED system with multiple giant atoms, *Optics Express* **32**, 9495 (2024).
- [97] Z.-M. Gao, J.-Q. Li, Z.-W. Li, W.-X. Liu, and X. Wang, Circuit QED with giant atoms coupling to left-handed superlattice metamaterials, *Physical Review A* **109**, 013716 (2024).
- [98] A. Gilchrist, N. K. Langford, and M. A. Nielsen, Distance measures to compare real and ideal quantum processes, *Physical Review A* **71**, 062310 (2005).
- [99] M.-D. Choi, Completely positive linear maps on complex matrices, *Linear Algebra and its Applications* **10**, 285 (1975).
- [100] F. W. Strauch, P. R. Johnson, A. J. Dragt, C. J. Lobb, J. R. Anderson, and F. C. Wellstood, Quantum Logic Gates for Coupled Superconducting Phase Qubits, *Physical Review Letters* **91**, 167005 (2003).
- [101] W. E. Lamb and R. C. Retherford, Fine structure of the hydrogen atom by a microwave method, *Phys. Rev.* **72**, 241 (1947).
- [102] For $N = 100$, the Hamiltonian Hilbert-space dimension is approximately 5500, implying a Liouvillian dimension of $5500^2 = 3.025 \times 10^7$, beyond the reach of current exact-diagonalization techniques.
- [103] J. Koch, T. M. Yu, J. Gambetta, A. A. Houck, D. I. Schuster, J. Majer, A. Blais, M. H. Devoret, S. M. Girvin, and R. J. Schoelkopf, Charge-insensitive qubit design derived from the Cooper pair box, *Physical Review A* **76**, 042319 (2007).
- [104] C. Mori, V. Milchakov, F. D'Esposito, L. Ruela, S. Kumar, V. N. Suresh, W. Ardati, D. Nicolas, G. Cappelli, A. Ranadive, G. L. Gal, M. Esposito, Q. Ficheux, N. Roch, T. Ramos, and O. Buisson, High-power readout of a transmon qubit using a nonlinear coupling (2025), [arXiv:2507.03642](https://arxiv.org/abs/2507.03642).
- [105] Z. Wang, R. W. Parker, E. Champion, and M. S. Blok, High- E_J/E_C transmon qubits with up to 12 levels, *Physical Review Applied* **23**, 034046 (2025).
- [106] S. J. de Graaf, S. H. Xue, B. J. Chapman, J. D. Teoh, T. Tsunoda, P. Winkel, J. W. O. Garmon, K. M. Chang, L. Frunzio, S. Puri, and R. J. Schoelkopf, A mid-circuit erasure check on a dual-rail cavity qubit using the joint-photon number-splitting regime of circuit QED, *npj Quantum Information* **11**, 1 (2025).
- [107] M. Kjaergaard, M. E. Schwartz, J. Braumüller, P. Krantz, J. I.-J. Wang, S. Gustavsson, and W. D. Oliver, Superconducting qubits: Current state of play, *Annual Review of Condensed Matter Physics* **11**, 369 (2020).
- [108] A. P. M. Place, L. V. H. Rodgers, P. Mundada, B. M. Smitham, M. Fitzpatrick, Z. Leng, A. Premkumar, J. Bryon, A. Vrajitoarea, S. Sussman, G. Cheng, T. Madhavan, H. K. Babla, X. H. Le, Y. Gang, B. Jäck, A. Gyenis, N. Yao, R. J. Cava, N. P. de Leon, and A. A. Houck, New material platform for superconducting transmon qubits with coherence times exceeding 0.3 milliseconds, *Nature Communications* **12**, 1779 (2021).
- [109] A. Somoroff, Q. Ficheux, R. A. Mencia, H. Xiong, R. Kuzmin, and V. E. Manucharyan, Millisecond Coherence in a Superconducting Qubit, *Physical Review Letters* **130**, 267001 (2023).
- [110] Y. Kim, A. Eddins, S. Anand, K. X. Wei, E. van den Berg, S. Rosenblatt, H. Nayfeh, Y. Wu, M. Zaletel, K. Temme, and A. Kandala, Evidence for the utility of quantum computing before fault tolerance, *Nature* **618**, 500 (2023).
- [111] J. Biznárová, A. Osman, E. Rehnman, L. Chayanun, C. Križan, P. Malmberg, M. Rommel, C. War-

- ren, P. Delsing, A. Yurgens, J. Bylander, and A. Fadavi Roudsari, Mitigation of interfacial dielectric loss in aluminum-on-silicon superconducting qubits, *npj Quantum Information* **10**, 78 (2024).
- [112] S. Kono, J. Pan, M. Chegnizadeh, X. Wang, A. Youssefi, M. Scigliuzzo, and T. J. Kippenberg, Mechanically induced correlated errors on superconducting qubits with relaxation times exceeding 0.4 ms, *Nature Communications* **15**, 3950 (2024).
- [113] M. Bal *et al.*, Systematic improvements in transmon qubit coherence enabled by niobium surface encapsulation, *npj Quantum Information* **10**, 43 (2024).
- [114] R. Acharya *et al.*, Quantum error correction below the surface code threshold, *Nature* **638**, 920 (2025).
- [115] S. Poorgholam-Khanjari, V. Seferai, P. Foshat, C. Rose, H. Feng, R. H. Hadfield, M. Weides, and K. Delfanazari, Engineering high-Q superconducting tantalum microwave coplanar waveguide resonators for compact coherent quantum circuit, *Scientific Reports* **15**, 27113 (2025).
- [116] T. Abad, J. Fernández-Pendás, A. Frisk Kockum, and G. Johansson, Universal Fidelity Reduction of Quantum Operations from Weak Dissipation, *Physical Review Letters* **129**, 150504 (2022).
- [117] T. Abad, Y. Schattner, A. F. Kockum, and G. Johansson, Impact of decoherence on the fidelity of quantum gates leaving the computational subspace, *Quantum* **9**, 1684 (2025).
- [118] T. Thorbeck, A. McDonald, O. Lanes, J. Blair, G. Keefe, A. A. Stabile, B. Royer, L. C. G. Govia, and A. Blais, High-fidelity gates in a transmon using bath engineering for passive leakage reset (2024), [arXiv:2411.04101](https://arxiv.org/abs/2411.04101).
- [119] X. Wang, J.-Q. Li, Z. Wang, A. F. Kockum, L. Du, T. Liu, and F. Nori, Nonlinear chiral quantum optics with giant-emitter pairs (2024), [arXiv:2404.09829](https://arxiv.org/abs/2404.09829).